© 2006 International Society of Nephrology

Acute sodium overload produces renal tubulointerstitial inflammation in normal rats

MI Rosón[1], S Cavallero[1], S Della Penna[1], G Cao[2], S Gorzalczany[1], M Pandolfo[1], A Kuprewicz[1], O Canessa[1], JE Toblli[2] and BE Fernández[1]

[1]*Cátedras de Fisiopatología Farmacologia Bioquímica Clínica y Anatomía Macro y Microscópica, Facultad de Farmacia y Bioquímica, Universidad de Buenos Aires and* [2]*Laboratory of Experimental Medicine, Hospital Aleman, Buenos Aires, Argentina*

The aim of the present study was to determine whether acute sodium overload could trigger an inflammatory reaction in the tubulointerstitial (TI) compartment in normal rats. Four groups of Sprague–Dawley rats received increasing NaCl concentrations by intravenous infusion. Control (C): Na^+ 0.15 M; G1: Na^+ 0.5 M; G2: Na^+ 1.0 M; and G3: Na^+ 1.5 M. Creatinine clearance, mean arterial pressure (MAP), renal blood flow (RBF), and sodium fractional excretion were determined. Transforming growth factor β1 (TGF-β1), α-smooth muscle actin (α-SMA), RANTES, transcription factor nuclear factor-kappa B (NF-κB), and angiotensin II (ANG II) were evaluated in kidneys by immunohistochemistry. Animals with NaCl overload showed normal glomerular function without MAP and RBF modifications and exhibited a concentration-dependent natriuretic response. Plasmatic sodium increased in G2 ($P<0.01$) and G3 ($P<0.001$). Light microscopy did not show renal morphological damage. Immunohistochemistry revealed an increased number of ANG II-positive tubular cells in G2 and G3, and positive immunostaining for NF-κB only in G3 ($P<0.01$). Increased staining of α-SMA in the interstitium ($P<0.01$), TGF-β1 in tubular cells ($P<0.01$), and a significant percentage ($P<0.01$) of positive immunostaining for RANTES in tubular epithelium and in glomerular and peritubular endothelium were detected in G3 > G2 > C group. These results suggest that an acute sodium overload is able '*per se*' to initiate TI endothelial inflammatory reaction (glomerular and peritubular) and incipient fibrosis in normal rats, independently of hemodynamic modifications. Furthermore, these findings are consistent with the possibility that activation of NF-κB and local ANG II may be involved in the pathway of this inflammatory process.

Kidney International advance online publication, 6 September 2006; doi:10.1038/sj.ki.5001831

KEYWORDS: renal tubulointerstitial inflammation; sodium overload; transforming growth factor; smooth muscle actin; RANTES

Correspondence: *MI Rosón, Cátedra de Fisiopatología, Facultad de Farmacia y Bioquímica, Universidad de Buenos Aires, Junín 956 5to. Piso, Buenos Aires C1113AAD, Argentina. E-mail: iroson@ffyb.uba.ar*

Received 15 March 2005; revised 13 December 2005; accepted 14 December 2005

It is well established that tubular sodium reabsorption is a major determinant of renal oxygen consumption,[1] and that renal tubular epithelial cell hypoxia associated with increased transport activity plays an important role in the development of structural damage in tubular cells.[2] Oxygen demand is well correlated with both tubular reabsorption and the glomerular filtration rate. The increase in either tubular reabsorption or glomerular filtration rate may impair the adequate renal oxygenation, favoring tubulointerstitial (TI) inflammation development.[3,4]

It has been reported that renal hypoxia upregulates adhesion molecules, cytokines, chemokines, leukocyte infiltration, and the production of reactive oxygen species (ROS).[5] In addition, increased ROS are known to act as second messengers in angiotensin II (ANG II) and transcription factor nuclear factor-kappa B (NF-κB) activation.[6] Recent reports indicate the importance of NF-κB activation in renal pathophysiology.[7,8] Transcription factor NF-κB plays a key role in the generation of proinflammatory cytokines as well as adhesion molecules.[9] Furthermore, NF-κB stimulates the angiotensinogen gene, which is the precursor for local ANG II production. Some studies have demonstrated that local production of ANG II in renal tissue is not related to circulating ANG II and it is not regulated by systemic hemodynamic changes.[10,11] Local ANG II is produced by tubular epithelial cells or macrophages at concentrations of 100- to 1000-fold higher than that of plasmatic ANG II. In this way, the local increase in ANG II levels may induce the expression of other proinflammatory genes, including chemokines (monocyte chemo attractant protein-1 and RANTES), cytokines (interleukin-6 and transforming growth factor β1 (TGF-β1)), adhesion molecules (vascular cell adhesion molecule-1 and intercellular adhesion molecule-1), and angiotensinogen. Consequently, local ANG II is responsible for the development of inflammatory responses in the heart, blood vessels, and kidney.[12–14] Increased local concentration of ANG II, which produces major TI inflammatory activity, enhances superoxide anion production by nicotinamide adenine dinucleotide phosphate (reduced form) oxidase activation.[15] As a result, a vicious feedback circle is generated between inflammation, oxidative stress, and ANG II production.[16] This evidence suggests that a

primary sodium overload offered to the tubular epithelial cells could be able to generate a cascade of events which starts with an increased oxygen demand and then, triggers overproduction of ROS, driving to local activation of ANG II and NF-κB. All these processes would initiate an inflammatory reaction expressed by cytokines (TGF-β1) and chemokines (RANTES). On this regard, studies using hypertensive rats have shown an altered distribution of the Na^+–K^+-ATPase in the proximal tubules, leading to a major sodium transport[17] and an incipient interstitial inflammation.[18]

Considering the important relationship between tubular epithelial sodium transport and renal oxygen consumption, the present study was performed in order to explore whether an acute sodium overload is able to trigger *per se* a TI inflammatory reaction in the kidney of normal rats, and whether this process is related to local ANG II participation and NF-κB activation.

RESULTS

To assess the effect of sodium overload in hemodynamic parameters, mean arterial pressure (MAP) and renal blood flow (RBF) were measured during the experimental period. The rats maintained their MAP and RBF levels within the normal range until the end of the experiment. In Table 1, measurements at 120 min are summarized. MAP levels in urethane-anesthetized rats appeared to be lower than those reported in anesthetized rats. Although these values are within the range reported by the literature,[19–21] it could be suggested that low arterial blood pressure could have limited possible RBF responses. However, in this case, it must also be considered that the decreased pressure must have affected the control and sodium overload groups in the same way.

In order to evaluate the effects of sodium load on glomerular function, urine and blood measurements of sodium and potassium were carried out and the results are summarized in Table 1. The urinary parameters shown correspond to the samples obtained along the last 30-min experimental period. After hypertonic saline solution overload, urinary flow increased in the three experimental groups in a concentration–response manner, reaching maximum values in G3. Urinary sodium concentration was higher in the three groups when compared with the control group, with no differences between them. Urinary potassium concentration also showed a concentration–response manner, reaching the maximum decrease in G3 group. Plasmatic sodium concentration increased in G2 and G3 groups. Plasmatic potassium concentration did not change significantly. In order to evaluate glomerular filtration rate, creatinine clearance (CC) was assessed. Sodium hypertonic infusion was unable to affect CC markedly in either group compared with the control group, but higher values in G2 compared with basal condition were observed ($P<0.05$) (Figure 1).

To further test whether changes in osmolality or in intracellular dehydration were related to sodium overload, plasmatic osmolality was measured and the degree of intracellular dehydration was calculated. Hypertonic sodium infusion displayed a mild dehydration (<5%) with no changes in plasmatic osmolality in G1 and G2. However, G3 had altered plasma osmolality ($P<0.05$) and also moderate intracellular dehydration (5–10%) (Table 1).

In order to establish the effect of sodium overload on the magnitude of sodium tubular transport changes, sodium fractional excretion (FE_{Na}) was measured. Data also allowed us to calculate filtered load and absolute sodium

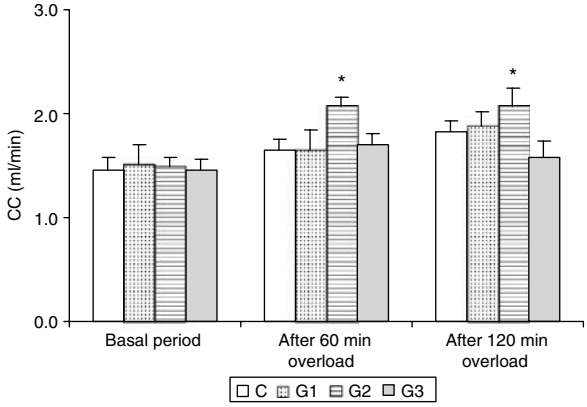

Figure 1 | CC. Control (C): Na^+ 0.15 M (ISS); G1: Na^+ 0.5 M, G2: Na^+ 1.0 M; and G3: Na^+ 1.5 M. *$P<0.05$ vs basal period. Values are expressed as mean ± s.e.m.

Table 1 | Urine and blood measurements

	C (n=7)	G1 (n=6)	G2 (n=7)	G3 (n=6)
Urinary Flow (μl min^{-1})	6.6±0.8	33.7±4.2*	105.1±15.3***	168.4±7.1***
Urinary Na^+ (mEq l^{-1})	51±11	309±19***	286±13***	291±6***
Plasmatic Na^+ (mEq l^{-1})	144±1	147±1	151±2**	159±2***
Urinary K^+ (mEq l^{-1})	246±16	129±19***	43±5***	36±2***
Plasmatic K^+ (mEq l^{-1})	2.9±0.1	2.7±0.1	2.8±0.1	3.3±0.1
Plasma Osmolality (mOsmol kg^{-1})	303±2	301±4	307±5	326±3***
Fractional excretion Na (%)	0.14±0.03	3.94±0.71***	10.07±0.69***	16.5±1.4***
Degree of intracellular dehydration (%)	0.1±0.3	1.9±0.6**	4.1±0.5***	6.5±0.2***
RBF (ml min^{-1})	8.3±1.5	9.3±1.5	8.4±0.8	8.8±0.8
MAP (mmHg)	77±2	76±5	77±3	81±3

MAP, mean arterial pressure; RBF, renal blood flow.
Values are mean ± s.e.m. *$P<0.05$; **$P<0.01$; ***$P<0.001$ vs Control.

reabsorption. As expected, FE_{Na} increased in a concentration–response manner after 120 min of sodium overload, being G3 > G2 > G1 (Table 1). In G2 and G3, sodium overload provoked an increase in filtered load at 60 min, whereas at 120 min, it was only enhanced in G2 ($P < 0.05$ vs C and $P < 0.01$ vs basal period) (Figure 2). At 60 min of sodium overload, absolute sodium tubular reabsorption was significantly increased ($P < 0.01$) in G2 and G3 in comparison to the basal period, meanwhile an overload for 120 min caused a significant ($P < 0.05$) increase in G2 (Figure 3).

The next goal was to study histological alterations through standard techniques for light microscopy, which did not show renal morphological damage in any group. Positive immunostaining in rats, loaded with hypertonic saline solution, are shown in Figures 4–8. No differences appeared in immunostaining in G1 when compared to the C group (data for α-smooth-muscle actin (α-SMA), TGF-β1, and RANTES not included). Measurement of interstitial α-SMA indicated a significative increment in G3 group compared with the control group (Figure 4), which suggests an incipient fibrotic process. Figure 5 demonstrates the presence of interstitial fibrosis characterized by an increase in the positive TI area for TGF-β1 found in G2 and G3 groups, being G3 > G2. Staining for RANTES increased in a

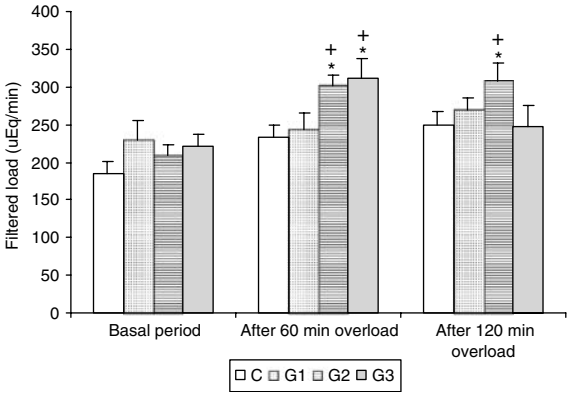

Figure 2 | Filtered load. Control (C): Na^+ 0.15 M (ISS); G1: Na^+ 0.5 M, G2: Na^+ 1.0 M; and G3: Na^+ 1.5 M. *$P < 0.05$; $^+P < 0.01$ vs basal period. Values are expressed as mean ± s.e.m.

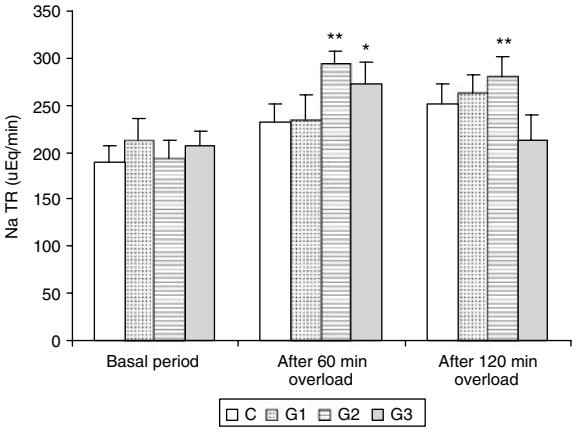

Figure 3 | Absolute sodium tubular reabsorption (NaTR). Control (C): Na^+ 0.15 M (ISS); G1: Na^+ 0.5 M, G2: Na^+ 1.0 M; and G3: Na^+ 1.5 M. *$P < 0.05$; **$P < 0.001$ vs basal period. Values are expressed as mean ± s.e.m.

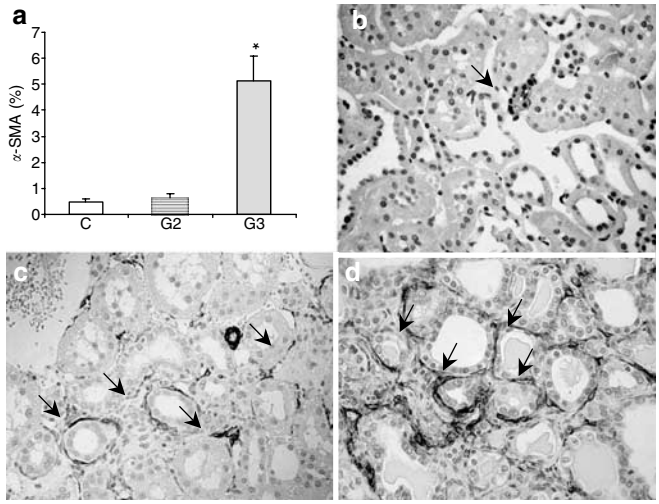

Figure 4 | Immunostaining of α-SMA in renal interstitium. (**a**) Quantitative representation of positive staining (except vessels)/mm^2, expressed as percentage ± s.d. Control (C): Na^+ 0.15 M (ISS); G2: Na^+ 1.0 M; and G3: Na^+ 1.5 M. *$P < 0.01$ vs control and G2. (**b**) Control group with α-SMA-positive staining just in vessels (arrow). (**c**) G2. Arrows indicate moderate positive staining in peritubular area. (**d**) G3. Note intense positive staining (arrows) in peritubular area (α-SMA, original magnification × 400).

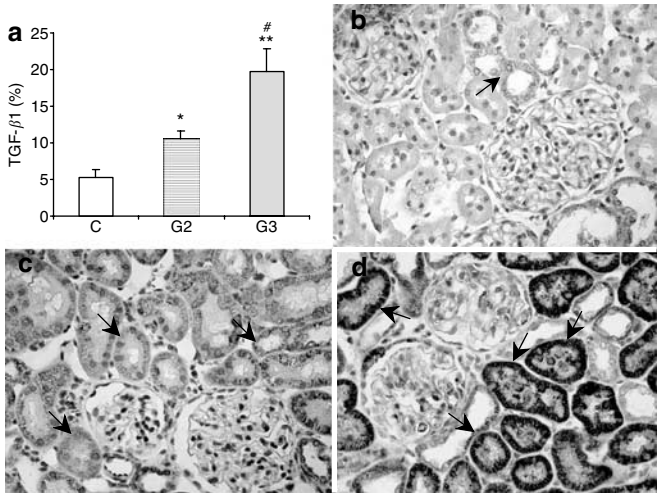

Figure 5 | Immunostaining of TGF-β1 in TI renal tissue. (**a**) Quantitative representation of positive staining/mm^2, expressed as percentage ± s.d. Control (C): Na^+ 0.15 M (ISS); G2: Na^+ 1.0 M; and G3: Na^+ 1.5 M. *$P < 0.05$; **$P < 0.01$ vs control; $^{\#}P < 0.05$ vs G2. (**b**) Control group with scanty TGF-β1-positive staining (arrow). (**c**) G2. Arrows indicate moderate positive staining. (**d**) G3. Note intense positive staining (arrows) in a large TI area (TGF-β1, original magnification × 400).

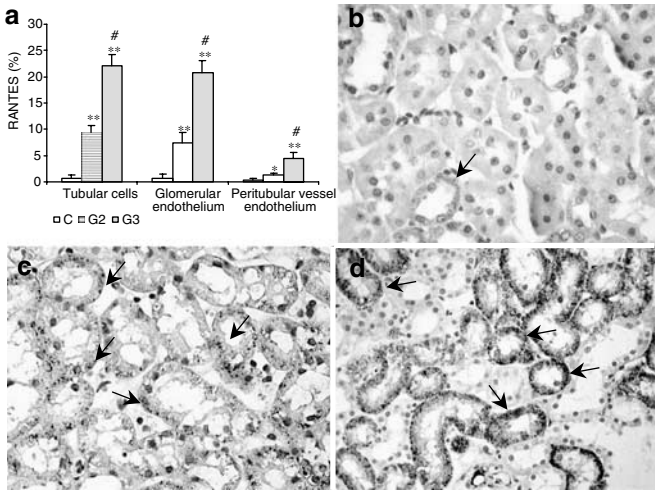

Figure 6 | Immunostaining of RANTES in renal tissue. (**a**) Quantitative representation of positive staining/mm^2, expressed as percentage ± s.d. Control (C): Na^+ 0.15 M (ISS); G2: Na^+ 1.0 M; and G3: Na^+ 1.5 M. *$P<0.05$; **$P<0.01$ vs control; $^{\#}P<0.01$ vs G2. (**b**) Control group with scanty positive staining (arrow) for RANTES. (**c**) G2. Arrows indicate moderate positive staining. (**d**) G3. Note intense positive staining (arrows) in a large TI area (RANTES, original magnification × 400).

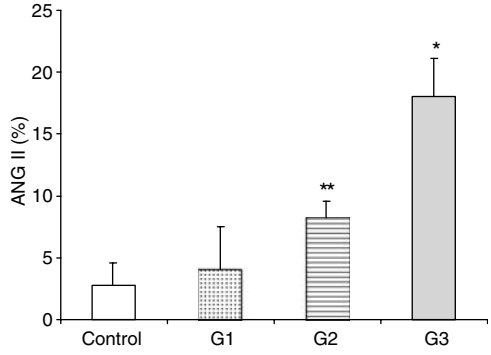

Figure 7 | Percentage of ANG II in renal tissue. Quantitative representation of positive immunostaining/mm^2, expressed as percentage ± s.d. Note that the increase in the expression of ANG II is dose dependent. Control (C): Na^+ 0.15 M (ISS); G1: Na^+ 0.5 M, G2: Na^+ 1.0 M; and G3: Na^+ 1.5 M. *$P<0.01$ vs all groups. **$P<0.01$ vs C and G1.

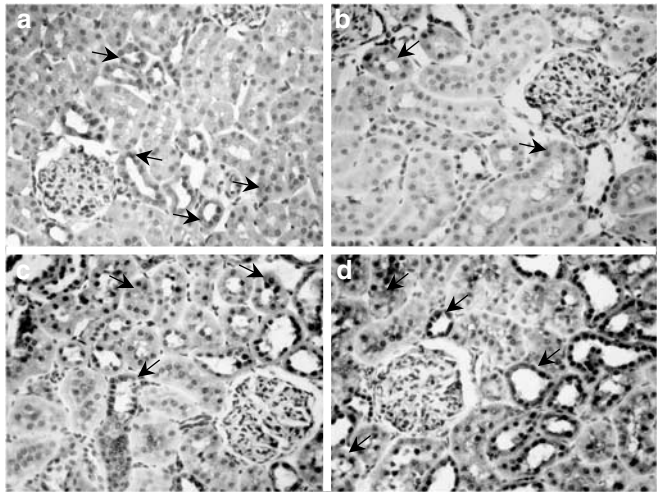

Figure 8 | Immunostaining of ANG II in renal tissue. (**a**) Control (C): Na^+ 0.15 M (ISS); (**b**) G1: Na^+ 0.5 M; (**c**) G2: Na^+ 1.0 M; and (**d**) G3: Na^+ 1.5 M. Arrows indicate positive staining for ANG II in tubular epithelial cells in the different groups (original magnification × 400).

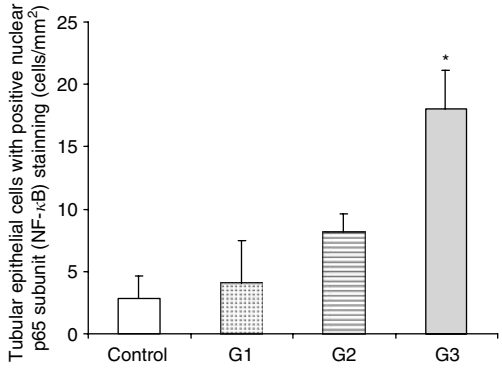

Figure 9 | Immunostaining of NF-κB in renal tissue. Quantitative representation of positive nuclear p65 subunit (NF-κB) cells/mm^2 ± s.d. Note that the increase in the expression of NF-κB is dose dependent. Control (C): Na^+ 0.15 M (ISS); G1: Na^+ 0.5 M, G2: Na^+ 1.0 M; and G3: Na^+ 1.5 M. *$P<0.01$ vs all groups.

concentration–response manner in glomerular endothelium, tubular cells, and in peritubular vessel endothelium, reaching maximum values in G3 group, as illustrated in Figure 6.

ANG II promotes proinflammatory transcription agents during hypoxia and inflammation.[13] Therefore, in order to establish a mechanism of inflammatory activation for sodium overload, we determined immunostaining of ANG II, which was markedly increased ($P<0.01$) in G2 in comparison to C and G1, and in G3 ($P<0.01$) in comparison with all groups (Figures 7 and 8).

To address the question whether NF-κB was involved in stimulation of chemokines and cytokines, the next goal was to study its immunohistochemistry. As illustrated in Figures 9 and 10, G3 showed a significative number of tubular epithelial cells with positive nuclear p65 subunit (NF-κB) staining when compared with the rest of the groups ($P<0.01$).

These changes in ANG II and NF-κB are parallel to the inflammatory process on epithelial tubular cells.

DISCUSSION

In the present study, kidneys of normal rats submitted to acute sodium overload showed the presence of early markers of TI inflammation, with a simultaneous increment of both transcription factor NF-κB and ANG II concentrations in tubular epithelial cells. This process was not accompanied by hemodynamic changes.

This experimental model characterized by saline overload showed undamaged glomerular function evidenced by

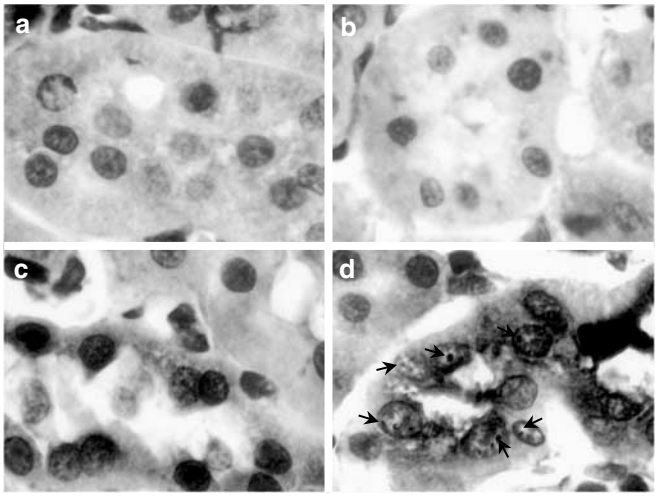

Figure 10 | Immunostaining of NF-κB in renal tissue. (**a**) Control (C): Na^+ 0.15 M (ISS); (**b**) G1: Na^+ 0.5 M; (**c**) G2: Na^+ 1.0 M; and (**d**) G3: Na^+ 1.5 M. Arrows indicate positive staining in nucleus of epithelial tubular cells for p65 subunit (NF-κB) only in G3 (original magnification × 1000).

normal or increased CC with no alterations in MAP and RBF, but exhibited an increased absolute sodium tubular reabsorption. Acute hypertonic saline overload generates a plasmatic volume expansion. As sodium is largely confined to the extracellular compartment, hypertonic saline overload expands the extracellular fluid space by extracting water from the cells. However, a rapid increase in plasma sodium concentration might produce salt poisoning. The diagnosis of salt poisoning is usually based on an increase in serum sodium concentration above 160 $mEq\,l^{-1}$.[22,23] In our study, even though plasmatic sodium was significantly greater in G2 and G3 groups as compared with the control group, it remained under 160 $mEq\,l^{-1}$ level in all groups. Plasmatic sodium levels corresponding to all the rats were within the reference normal range for plasma sodium concentration; therefore, rats were not exposed to risk for the adverse effects of hypernatremia. It must be remarked that plasma osmolality rose only in G3 group, but at a degree that did not exceed the physiological level induced by mild to moderate dehydration.[24] In agreement to this, histopathological studies did not evidence morphological renal damage. These results let us characterize a model for acute sodium overload in rats, which exhibited increased filtered load and greater sodium tubular reabsorption accompanied by preserved glomerular function and tubular morphology. This model allowed us the study of early TI inflammatory modifications before functional and/or structural changes appeared.

The presence of immunostaining for inflammatory markers in our study was in agreement with the progressive sodium overload and increasing FE_{Na} (G3 > G2 > G1).

TGF-β1 is a member of a family of five polypeptides that exert complex effects on organ development, cell growth and differentiation, expression of extracellular matrix and proteins, immune responses, angiogenesis, and tissue repair. Their biological effects depend on the target cell, the degree of cellular differentiation, and cellular environment.[25] α-SMA is a smooth muscle cell cytoskeleton protein and a marker of trans-differentiation from fibroblast to myofibroblast. In normal kidneys, α-SMA is present only in adventitia and vascular media whereas, during the fibrotic process, cells that express α-SMA are detected in renal interstitium. RANTES is a chemokine synthesized by epithelial and endothelial cells, as well as macrophages that contribute to massive recruitment of neutrophils and eosinophils to the inflammatory site.

In this study, a positive staining for RANTES, detected in tubular epithelium and glomerular and peritubular endothelium at high NaCl overload, represents an early and clear index of acute inflammation. Furthermore, we observed a positive staining for TGF-β1, which impacts principally at tubules in renal cortex and medulla. This could denote the development of an early process of inflammation and incipient fibrosis. TGF-β1 is one of the most important candidates for ANG II-mediated matrix synthesis.[26] Experimental studies in kidney demonstrated the increasing TGF-β1 associated with locally enhanced ANG II and extracellular matrix proteins that diminished by angiotensin-converting enzyme inhibition.[27,28] TGF-β1 activation upregulates a cellular volume-sensitive kinase named hSGK1, which stimulates epithelial sodium channels.[29] Then, an increase in sodium inflow is able to promote a cascade characterized by enhanced cell swelling, which leads to proteolysis inhibition and increased protein synthesis and develops, in turn, excessive extracellular matrix expansion. We demonstrated positive staining for α-SMA in renal peritubular interstitium only at the highest concentration of NaCl infusion. The accumulation of myofibroblasts, which express α-SMA leading to extracellular matrix expansion, constitutes an early event in interstitial fibrogenesis. It was demonstrated that protein overload upregulates fibrogenic and proinflammatory TGF-β1 expression in proximal tubules and in interstitial cells. α-SMA is strongly upregulated by TGF-β1 in the tubulointerstitial area and appears to play a role in the transformation of fibroblasts into myofibroblasts.[30] This is in agreement with the most intense staining of TGF-β1 in tubular epithelium.

The mechanisms by which hypertonic sodium is able to develop inflammatory reaction must be defined. It has been described that renal epithelial cells react in the presence of increased hypoxia, hyperosmolarity, or intracellular dehydration with increased production of ROS, NF-κB activation, and mitogen-activated protein kinases signaling mechanisms increment.[31,32] Considering that in our experiment there probably exists hypoxia according to a major oxygen demand related to the increase in sodium transporting activity, it could be suggested that hypoxia could be triggering an increase in ROS and a concomitant increment in NF-κB and ANG II activation. One possibility to be considered is that sodium overload increases local renin–angiotensin system

and activates NF-κB through an increment in ROS production.[6] ANG II, in turn, is able to stimulate NF-κB expression, being this effect mediated by ANG II type 1 and ANG II type 2 receptors in the kidney.[33] Furthermore, NF-κB activation stimulates cytokines, chemokines, and the angiotensinogen gene. These processes could provide a positive feedback mechanism that upregulates ANG II production. In the present study, we have observed a positive staining for ANG II and transcription factor NF-κB in rats with acute saline overload, a model well characterized by a depressed plasmatic renin activity.[34] This fact constitutes further evidence that intrarenal ANG II is regulated independently of systemic ANG II and that its increase could be related to the outcome of an inflammatory process in tubular epithelium. Nevertheless, an increase in osmolality cannot be ruled out, and in this way, the moderate intracellular degree of dehydration observed in G3 can also be a cause for NF-κB activation. Recent evidence has implicated NF-κB as an important osmosignaling molecule that is activated in response to hyperosmolarity in both renal medullar interstitial and endothelial cell.[35–38] In addition, dehydration activates NF-κB in renal medullar interstitial cells.[39] Therefore, the injury observed in G3 may not specifically be a consequence of the excessive tubular sodium reabsorption. It is possible that hyperosmolarity and moderate dehydration may be more important to explain the changes observed in this group. Our results, taken together with the antecedents mentioned above, support the possibility that increased activation of NF-κB and expression of ANG II could contribute to inflammatory process developed after an acute sodium overload.

The model of hypertonic expansion could be useful for the analysis of the therapeutic effects of anti-inflammatory agents. Therefore, further studies to evaluate strategies for salt-sensitive hypertension treatment should be considered, not only for the use of drugs that lower blood pressure, but also for the control of renal interstitial inflammation. Most of our results show a sodium concentration-dependent response this indicating that renal acute inflammation is initiated by sodium overload, and suggesting an active participation of sodium and hyperosmolarity in the pathogenesis of the inflammatory process.

In conclusion, an acute sodium overload is capable '*per se*' of triggering endothelial inflammatory reaction (glomerular and peritubular) and TI incipient fibrosis in normal rats with preserved kidney function and intact renal morphology. Furthermore, these findings are consistent with the possibility that activation of NF-κB and ANG II may be involved in the inflammatory process. Our data provide insight into the inflammatory process during acute sodium overload not associated with hemodynamic alterations.

Considering that the acute renal injury depends on the extent of the hypoxic stress, present results could be of interest for the use of early markers of inflammation and fibrosis before functional and structural changes appear.

MATERIALS AND METHODS

Experiments were performed in adult male Sprague–Dawley rats, 270–350 g body weight (BW), housed at controlled temperature ($23 \pm 2^{\circ}C$) and exposed to a daily 12-h light–dark cycle (lights on 7:00 AM to 7:00 PM) with free access to tap water and standard rat chow.

On the day of the experiment, rats were anesthetized with urethane 10% intraperitoneally ($1.2\,g\,kg^{-1}$ BW), a tracheotomy was performed, and a polyethylene-90 tubing (3 cm long) was inserted into the trachea to maintain an open airway. The left femoral vein was catheterized with a Silastic cannula (0.12 mm intradermal) for continuous intravenous infusion. The right carotid artery was also catheterized with T4 tubing for blood sampling and continuous blood pressure monitoring. MAP was measured by connecting the carotid artery catheter to a pressure transducer Statham GOULD P23ID coupled to a Grass Polygraph 79D. The bladder was cannulated for urine collection using a polyethylene-75 cannula.

All infusions were carried out at the same rate of $0.4\,ml\,min^{-1}$ (Syringe Infusion Pump, Sage™, Orion Research Inc., Orion, USA). A 45-min infusion with isotonic saline solution (ISS) was allowed to reach a steady-state diuresis to allow urine collection. Then, a basal period of 60-min infusion of ISS was carried out. After that, NaCl was administered to each group for 120 min at different concentrations: Control (C): Na^+ 0.15 M (ISS); G1: Na^+ 0.5 M; G2: Na^+ 1.0 M; and G3: Na^+ 1.5 M. These concentrations corresponded to the following doses: C: $0.12\,mEq\,h^{-1}100g^{-1}$ BW; G1: $0.40\,mEq\,h^{-1}100\,g^{-1}$ BW; G2: $0.80\,mEq\,h^{-1}100\,g^{-1}$ BW; and G3: $1.20\,mEq\,h^{-1}100\,g^{-1}$ BW. The total volume infused in each rat was 9 ml. Urine and blood samples were collected every 30 and 60 min, respectively, for sodium, potassium, osmolality, and creatinine measurements. MAP was recorded every 30 min. In order to evaluate renal plasmatic flow, sodium para-aminohippurate was given by infusion at a concentration of 0.5%.

Urine and blood measurements

Urine volume was determined by gravimetry, assuming urine density as 1.0 g/ml. Sodium, potassium, and creatinine in urine and plasma samples were measured by standard methods. Plasma osmolality was determined by freezing-point depression. FE_{Na}, CC, and para-aminohippurate clearance were calculated according to standard formula. Urine flow is expressed as μl/min, plasmatic and urinary Na^+ and K^+ as mEq/l, plasma osmolarity as mOsmol/kg, CC as ml/min, and FE_{Na} as the percentage (%) of filtrated sodium. Para-aminohippurate clearance was calculated for estimation of renal plasmatic flow. RBF was calculated as: renal plasmatic flow/(1-hematocrit).

Kidney processing and examination

At the end of the infusion period, the left kidney was perfused with ISS through the abdominal aorta, until the blood was washed out and the parenchyma presented a pale appearance. The kidney was rapidly excised, decapsulated, cut longitudinally, and harvested for light microscopy and immunohistochemical studies.

Light microscopy and immunolabeling

Tissues were fixed in phosphate-buffered 10% formaldehyde (pH 7.2) and embedded in paraffin using conventional histological techniques. Three-micron sections were cut and stained with hematoxylin-eosin and Masson's Trichrome. Paraffin sections were cut at 3 μm, deparaffined, and rehydrated. Endogenous peroxidase

activity was blocked by treating with 0.5% H_2O_2 in methanol for 30 min. Local ANG II was detected using an anti-human antibody (Peninsula, CA, USA) at a dilution of 1:200. In order to evaluate the inflammatory response, the following antibodies were used: monoclonal and goat polyclonal immunoglobulin G anti-NF-κB p65 (sc-8008 Santa Cruz Biotechnology Inc., Santa Cruz, CA, USA) at a dilution of 1:150, anti-TGF-β_1 (Santa Cruz Biotechnology Inc.) at a dilution of 1:100, a mouse anti-α-SMA (Sigma Chemical Co., St Louis, MO, USA) at a dilution of 1:100, and a goat polyclonal immunoglobulin G anti-RANTES (sc-1410 Santa Cruz Biotechnology Inc.) at a dilution of 1:100.

Immunostaining was carried out using a commercially modified avidin–biotin–peroxidase complex technique, Vectastain ABC kit (Universal Elite, Vector Laboratories, CA, USA), and counterstained with hematoxylin. The samples were handled as described previously.[40]

Morphological analysis

Histological sections were studied in each animal using a light microscope Nikon E400 (Nikon Instrument Group, Melville, NY, USA). Ten consecutive microscopic fields ($\times$ 400 magnification) by sample were analyzed to evaluate morphological changes in glomeruli and tubules, as well as in the renal interstitium. All measurements were carried out using an image analyzer Image-Pro Plus version 4.5 for Windows (Media Cybernetics, LP. Silver Spring, MD, USA).

Statistical analysis

The assumption test to determine the Gaussian distribution was performed by the Kolmogorov and Smirnov method. For parameters with Gaussian distribution, all the comparisons among groups were carried out using analysis of variance followed by the Newman–Keuls test. Results from urine and blood samples and MAP levels are expressed as mean $\pm$ s.e.m. Statistical analysis for those parameters like histological data with non-Gaussian distribution was performed by Kruskal–Wallis test (nonparametric analysis of variance) and Dunn's multiple comparison test; using absolute values and processed through GraphPad Prism, version 2.0 (GraphPad Software Inc., San Diego, CA, USA). Presence of α-SMA, TGF-β1, and RANTES are expressed as mean of percentages of positive staining area/mm^2 $\pm$ s.d. A value of $P<0.05$ was considered to be significant.

REFERENCES

1. Brezis M, Heyman SN, Epstein FH. Determinants of intrarenal oxygenation. II. Hemodynamic effects. *Am J Physiol* 1994; **267**(Part 2): F1063–F1068.
2. Brezis M, Rosen S. Hypoxia of the renal medulla. Its implications for disease. *N Engl J Med* 1995; **332**: 647–655.
3. Brezis M, Rosen S, Silva P *et al.* Transport activity modifies thick ascending limb damage in the isolated perfused kidney. *Kidney Int* 1984; **25**: 65–72.
4. Swärd K, Valsson F, Sellgren J *et al.* Differential effects of human atrial natriuretic peptide and furosemide on glomerular filtration rate and renal oxygen consumption in humans. *Int Care Med* 2005; **31**: 79–85.
5. Rodriguez-Iturbe B, Quiroz Y, Herrera-Acosta J *et al.* The role of immune cells infiltrating the kidney in the pathogenesis of salt-sensitive hypertension. *J Hypertens* 2002; **20**(Suppl 3): S9–S14.
6. Schreck R, Rieber P, Baeuerle PA. Reactive oxygen intermediates as apparently widely used messengers in the activation of the NF-κB transcription factor and HIV. *EMBO J* 1991; **10**: 2247–2258.
7. Jobin C, Sartor RB. The I kappa B/NF-kappa B system: a key determinant of mucosal inflammation and protection. *Am J Physiol Cell Physiol* 2000; **278**: C451–C462.
8. Zoja C, Donadelli R, Colleoni S *et al.* Protein overload stimulates RANTES production by proximal tubular cells depending on NF-kappa B activation. *Kidney Int* 1998; **53**: 1608–1615.
9. Tak PP, Firestein GS. NF-κB. A key role in inflammatory diseases. *J Clin Invest:* 2001; **107**: 7–11.
10. Nishiyama A, Masanori Y, Matlubur R *et al.* Effects of AT1 receptor blockade on renal injury and mitogen-activated protein activity in Dahl salt-sensitive rats. *Kidney Int* 2004; **65**: 972–981.
11. Cambell DJ, Lawrence AC, Towrie A *et al.* Differential regulation of angiotensin levels in plasma and kidney of the rat. *Hypertension* 1991; **18**: 763–773.
12. Rodriguez-Iturbe B, Pons H, Quiroz Y *et al.* Mycophenolate mofetil prevents salt-sensitive hypertension resulting from angiotensin II exposure. *Kidney Int* 2001; **59**: 2222–2232.
13. Ruiz-Ortega M, Ruperez M, Lorenzo O *et al.* Angiotensin II regulates the synthesis of proinflammatory cytokines and chemokines in the kidney. *Kidney Int* 2002; **82**(Suppl): 12–22.
14. Klahr S, Morrissey JJ. Angiotensin II and gene expression in the kidney. *Am J Kidney Dis* 1998; **31**: 171–176.
15. Rajagopalan S, Kurz S, Munzel T *et al.* Angiotensin II-mediated hypertension in the rat increases vascular superoxide production via membrane NADH/NADPH oxidase activation: contribution to alterations of vasomotor tone. *J Clin Invest* 1996; **97**: 1916–1923.
16. Rodriguez-Iturbe B, Vaziri ND, Herrera-Acosta J *et al.* Oxidative stress, renal infiltration of immune cells, and salt-sensitive hypertension: all for one and one for all. *Am J Physiol Renal* 2004; **286**: F606–F616.
17. Hinojos CA, Doris PA. Altered subcellular distribution of Na^+, K^+-ATPase in proximal tubules in young spontaneously hypertensive rats. *Hypertension* 2004; **44**: 95–100.
18. Rodriguez-Iturbe B, Quiroz Y, Ferrebuz A *et al.* Evolution of renal interstitial inflammation and NF-κB activation in spontaneously hypertensive rats. *Am J Nephrol* 2004; **24**: 587–594.
19. Jochem J, Zwirska-Korczala K, Gwozdz B *et al.* Cardiac and regional haemodynamic effects of endothelin-1 in rats subjected to critical haemorrhagic hypotension. *J Physiol Pharmacol* 2003; **54**: 383–396.
20. Azad A, Lall SB, Mittra S. Effect of *N*-acetylcysteine and L-NAME on aluminium phosphide induced cardiovascular toxicity in rats. *Acta Pharmacol Sin* 2001; **22**: 298–304.
21. Butcher KS, Cecheto DF. Insular lesion evokes autonomic effects of stroke in normotensive and hypertensive rats. *Stroke* 1995; **26**: 459–465.
22. Ajito T, Suzuki K, Iwabuchi S. Effect of intravenous infusion of a 7.2% hypertonic saline solution on serum electrolites and osmotic pressure in healthy beagles. *J Vet Med Sci* 1999; **6**: 637–641.
23. Tyler JW, Welles EG, Sorjonen DC *et al.* Cerebrospinal fluid composition of cattle with endotoxin-induced mastitis treated with isotonic (0.9%) or hypertonic (7.5%) sodium chloride. *J Vet Int Med* 1993; **7**: 91–94.
24. Oliveira GR, Franci CR, Rodovalho GV *et al.* Alterations in the central vasopressin and oxytocin axis after lesion of a brain osmotic sensory region. *Brain Res Bull* 2004; **63**: 515–520.
25. Kondo S, Kagami S, Urushihara M *et al.* Transforming growth factor-beta1 stimulates collagen matrix remodeling through increased adhesive and contractive potential by human renal fibroblasts. *Biochim Biophys Acta* 2004; **1693**: 91–100.
26. Border WA, Noble NA. Interaction of transforming growth factor-beta and angiotensin II in renal fibrosis. *Hypertension* 1998; **31**: 181–188.
27. Mezzano SA, Ruiz-Ortega M, Egido J. Angiotensin II in renal fibrosis. *Hypertension* 2001; **38**: 635–638.
28. Ruiz-Ortega M, Gonzalez S, Seron D *et al.* ACE inhibition reduces proteinuria, glomerular lesions and extracellular matrix production in a normotensive rat model of immune complex nephritis. *Kidney Int* 1995; **48**: 1778–1791.
29. Warntges S, Grone HJ, Capasso G *et al.* Cell volume regulatory mechanisms in progression of renal desease. *N Nephrol* 2001; **14**: 319–326.
30. Gupta S, Clarkson MR, Duggan J *et al.* Connective tissue growth factor: potencial role in glomerulosclerosis and tubulointerstitial fibrosis. *Kidney Int* 2000; **58**: 1389–1399.
31. Haussinger D, Schliess F, Dombrowski F *et al.* Involvement of p38MAPK in the regulation of proteolysis by liver cell hydration. *Gastroenterology* 1999; **116**: 921–935.
32. Németh ZH, Deitch EA, Czabó C *et al.* Hyperosmotic stress induces nuclear factor-éB activation and interleukin-8 production in human intestinal epithelial cells. *Am J Pathol* 2002; **161**: 987–996.
33. Esteban V, Lorenzo O, Ruperez M *et al.* Angiotensin II, via AT1 and AT2 receptors and NF-kappa B pathway, regulates the inflammatory in unilateral uretral obstruction. *J Am Soc Nephrol* 2004; **15**: 1514–1529.

34. Amadieu-Farmakis M, Giry J, Barlet JP. Increase in plasma concentration of atrial natriuretic peptide during infusion of hypertonic saline in conscious newborn calves. *J. Endocrinol* 1988; **119**: 23–29.
35. Loitsch SM, von Mallinckrodt C, Kippenberger S *et al*. Reactive oxygen intermediates are involved in IL-8 production induced by hyperosmotic stress in human bronchial epithelial cells. *Biochem Biophys Res Commun* 2000; **276**: 571–578.
36. Yorek MA, Dunlap JA, Liu W *et al*. Normalization of hyperosmotic-induced inositol uptake by renal and endothelial cells is regulated by NF-κB. *Am J Physiol* 2000; **278**: C1011–C1018.
37. Haussinger D, Schliess F. Osmotic induction of signaling cascades: role in regulation of cell function. *Biochem Biophys Res Commun* 1999; **255**: 551–555.
38. Kultz D. Hyperosmolality triggers oxidative damage in kidney cells. *Proc Natl Acad Sci USA* 2004; **101**: 9177–9178.
39. Hao CM, Yull F, Blackwell T *et al*. Dehydration activates an NF-κB driven COX2-dependent survival mechanism in renal medullary interstitial cells. *J Clin Invest* 2000; **106**: 973–982.
40. Hsu SM, Raine L, Fanger H. Use of avidin–biotin–peroxidase complex (ABC) immunoperoxidase techniques: a comparison between ABC and unlabeled antibody (PAP) procedures. *J Histochem Cytochem* 1981; **29**: 577–580.